DALTON
FULL PAPER

One- and two-dimensional materials containing vanadium oxide: structures and magnetic properties of $Cu(dien)V_2O_6·H_2O$ and $Ni(dien)V_2O_6$ (dien = diethylenetriamine)†

Li-Min Zheng,*[a] Jie-Shou Zhao,[a] Kwang-Hwa Lii,[b] Li-Yi Zhang,[a] Yang Liu[a] and Xin-Quan Xin[a]

[a] *State Key Laboratory of Coordination Chemistry, Coordination Chemistry Institute, Nanjing University, Nanjing 210093, China. E-mail: lmzheng@netra.nju.edu.cn. Fax: +86-25-3314502*
[b] *Institute of Chemistry, Academia Sinica, Taipei, China*

Received 12th November 1998, Accepted 21st January 1999

The structures of a one-dimensional compound $Cu(dien)V_2O_6·H_2O$ **1** and a two-dimensional compound $Ni(dien)V_2O_6$ **2**, where dien is diethylenetriamine, have been determined by X-ray diffraction. The former is composed of corner-sharing VO_4 tetrahedra chains, with $Cu(dien)^{2+}$ fragments attached to every other VO_4 unit. The latter has a layer structure with the V_4O_{12} tetramers connected by edge-shared $Ni_2(\mu\text{-}O)_2(dien)_2^{4+}$ dimers. The layers are further stacked to form one-dimensional channels along the [001] direction. Magnetic susceptibility measurements for both compounds have been performed down to 2 K. Paramagnetic behavior is observed in **1**, whereas ferromagnetic interaction is found to be dominant in **2**.

Although the vanadium oxides have been well documented to exhibit interesting intercalation, electronic and magnetic properties, it is only recently that attention has been drawn to the synthesis and structure of such new compounds that are templated by organic amines.[1–8] Examples of the vanadium oxides templated or co-ordinated by transition metal complexes, however, are still rare. They include one-dimensional metavanadate chain compounds $Cu(NH_3)_2V_2O_6$,[9] $Cu(en)V_2O_6$, $Cu(bipy)V_2O_6$ and $Cu(bipy)_2V_2O_6$,[10] where the co-ordination groups are attached to the V–O chains. Layered mixed-valence vanadium oxides have also been found in $[Cu(en)_2][V_6O_{14}]$, $[Cu(en)_2]_2[V_{10}O_{25}]$, $[Zn(bipy)_2]_2[V_6O_{17}]$ and $[Zn(en)_2][V_6O_{14}]$,[11] where the copper(II) or zinc(II) complexes reside between V–O layers as charge compensating templates. Owing to the ability of vanadium to adopt a variety of co-ordination geometries in various oxidation states, the influences of the second metal ions as well as the organic ligands on the structures could be significant. Therefore, novel structural types could be discovered by modifying the transition metal ions, the organic groups and the synthetic conditions, *etc*.

On the other hand, the vanadium oxides which contain transition metal complexes may be of interest in molecular magnetism. A variety of magnetic clusters with different kinds of interacting ions and increasing nuclearities may be obtained which are well isolated by the diamagnetic vanadium oxides, and thus allow for a detailed investigation of their magneto-structural relationships.

In this paper we report the hydrothermal syntheses, structures and magnetic properties of a chain compound $Cu(dien)V_2O_6·H_2O$ **1** and a layer compound $Ni(dien)V_2O_6$ **2** (dien = diethylenetriamine).

Experimental

Materials and methods

All reagents were obtained from commercial sources and used as purchased. The elemental analyses were performed on a PE 240C elemental analyzer. The infrared spectra were recorded on a IFS66V FT-IR spectrophotometer with pressed KBr pellets. Powder X-ray diffraction was carried out on a Rigaku D/Max-RA diffractometer. Powder X-band EPR spectra were recorded at room temperature with a FE1XG ESR spectrometer. Variable-temperature magnetic susceptibility data were obtained on polycrystalline samples (14.2 mg for compound **1** and 22.8 mg for **2**) from 2 to 300 K in a magnetic field of 5 kG after zero-field cooling using a SQUID magnetometer. Diamagnetic corrections were estimated from Pascal's constants. The temperature independent paramagnetism was taken as 60×10^{-6} cm^3 mol^{-1} for the copper(II) monomer and 100×10^{-6} cm^3 mol^{-1} for the nickel(II) monomer.

Syntheses

$Cu(dien)V_2O_6·H_2O$ 1. A mixture of NH_4VO_3 (0.2346 g, 2.0 mmol), $Cu(NO_3)_2·3H_2O$ (0.2421 g, 1.0 mmol), NH_4F (0.0601 g, 1.0 mmol), dien (0.1 mL, 1.0 mmol) and water (10 mL) was heated with stirring for 1.5 h. The mixture was then transferred to a Teflon-lined autoclave (25 mL) and kept at 140 °C for 40 h. After slow cooling, black needle-like crystals appeared as a major phase, together with a small amount of an unidentified green powder. The black needles were manually selected for the structural determination and measurement of the bulk properties (Found: C, 12.40; H, 3.74; N, 10.53. Calc.: C, 12.55; H, 3.92; N, 10.98%). IR (KBr): 3414m, 3391m, 3306w, 3242m, 3145w, 3121m, 2966w, 2923w, 2879w, 1653w, 1606w, 1586w, 1452w, 1394w, 1260w, 1162w, 1140w, 1100m, 1032m, 934s, 911s, 881m, 857m, 828s, 713m, 638s, 589m, 521w, 467w and 424w cm^{-1}.

$Ni(dien)V_2O_6$ 2. Compound **2** was synthesized as brown microcrystals by heating a mixture of NH_4VO_3 (0.2340 g, 2.0 mmol), $NiSO_4·7H_2O$ (0.2873 g, 1.0 mmol), dien (0.1 mL, 1.0 mmol) and water (10 mL) at 140 °C for 40 h. The monophasic character was judged by powder X-ray diffraction, by comparison with the pattern derived from single crystal data. Single crystals suitable for the structural determination were obtained by hydrothermal treatment of a mixture of NH_4VO_3 (0.4680 g, 4.0 mmol), $NiSO_4·7H_2O$ (0.2812 g, 1.0 mmol), dien (0.1 mL, 1.0

† *Supplementary data available*: IR and EPR spectra, XRD patterns. Available from BLDSC (No. SUP 57492, 6 pp.). See Instructions for Authors, 1999, Issue 1 (http://www.rsc.org/dalton).

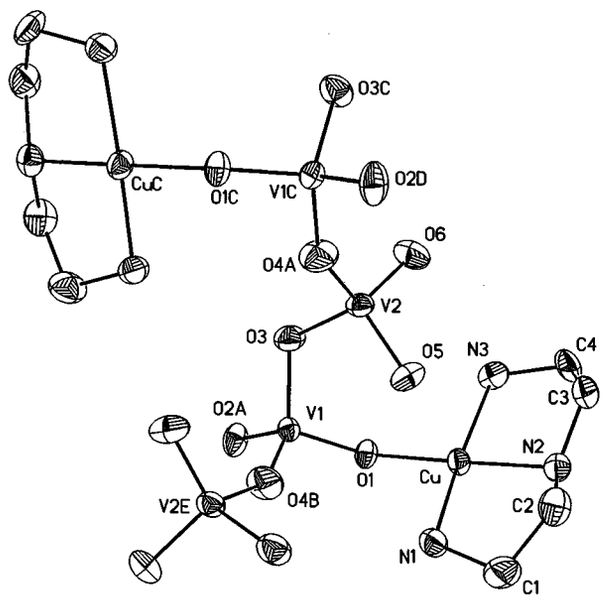

Fig. 1 A fragment of the chain with the atomic labeling scheme (50% probability) in compound **1**. The hydrogen atoms are omitted for clarity.

mmol) and water (10 mL) at 140 °C for 40 h (Found: C, 13.39; H, 3.75; N, 11.34. Calc.: C, 13.35; H, 4.17; N, 11.68%). IR (KBr): 3306m, 3270m, 3250m, 3159w, 2965w, 2936w, 2881w, 1590w, 1035w, 967m, 932w, 879m, 805s, 767s, 660w, 607w, 547w, 516w and 475w cm^{-1}.

X-Ray crystallographic analysis

Crystal structure determinations for compounds **1** and **2** were performed on a Siemens Smart-CCD diffractometer equipped with a normal focus, 3 kW sealed tube X-ray source and graphite-monochromated Mo-Kα radiation ($\lambda = 0.71073$ Å) at 293 K. Some relevant crystallographic data and structure determination parameters are listed in Table 1. Intensity data were collected in 1200 frames for **1** and 2082 frames for **2** with increasing ω (width of 0.30° per frame). Empirical absorption corrections were applied by using the SADABS program for the Siemens area detector. The structures were solved by direct methods and refined by using SHELXTL.[12] All non-hydrogen atoms in both structures were refined with anisotropic displacement parameters. All hydrogen atoms were localized in difference electron density maps and refined with variable positional and isotropic displacement parameters for **1** and **2**. Selected bond lengths and angles are given in Table 2 for **1** and Table 3 for **2**.

CCDC reference number 186/1329.

See http://www.rsc.org/suppdata/dt/1999/939/ for crystallographic files in .cif format.

Results and discussion

Crystal structure of $Cu(dien)V_2O_6 \cdot H_2O$ 1

The structure of compound **1** consists of corner-sharing VO_4 tetrahedra chains running along the *a* axis, with the Cu(dien) moieties covalently attached to every other vanadium site through oxygen atoms. Fig. 1 depicts a fragment of the chain together with the atomic labeling scheme.

Within the chain there are two crystallographically distinct vanadium atoms V(1) and V(2) which are bridged by O(3) and O(4). Both vanadium atoms have distorted tetrahedral environments. The bond distances of the bridging oxygen and the vanadium atoms range from 1.766(3) to 1.838(3) Å. The values are comparable to those in $Cu(en)V_2O_6$ and $Cu(bipy)V_2O_6$ [1.779(3)–1.794(4) Å] and in $Cu(bipy)_2V_2O_6$ [1.775(3)–1.837(3) Å].[10] The V(1) atom further connects with the Cu(dien) fragment through the O(1) atom. The V(1)-O(1) length is 1.687(3) Å which is in agreement with that in $Cu(bipy)_2V_2O_6$ [1.678(5) Å]. The remaining terminal oxygen atoms have V–O distances between 1.622(3) and 1.640(3) Å which agree well with those of other metavanadates.

Table 1 Crystal data for compounds **1** and **2**

	1	**2**
Formula	$C_4H_{15}CuN_3O_7V_2$	$C_4H_{13}N_3NiO_6V_2$
M	382.61	359.76
Space group	$P2_12_12_1$	$P\bar{1}$
a/Å	8.014(2)	7.3770(1)
b/Å	9.703(2)	8.0930(1)
c/Å	16.230(3)	10.2350(1)
α/°		101.807(1)
β/°		102.801(1)
γ/°		98.831(1)
V/Å^3	1262.08(9)	570.46(1)
Z	4	2
D_c/g cm^{-3}	2.014	2.094
F(000)	764	360
μ(Mo-Kα)/cm^{-1}	31.45	32.53
Maximum 2*θ*/°	57.7	55.94
Reflections collected	7919	5431
Independent reflections	3042 ($R_{int} = 0.0475$)	2460 ($R_{int} = 0.0348$)
T_{min}, T_{max}	0.585, 0.879	0.789, 0.956
Data, restraints, parameters	3042, 0, 214	2460, 0, 198
Goodness of fit on F^2	0.987	1.049
*R*1, *wR*2 [$I > 2\sigma(I)$]	0.0369, 0.0649	0.0290, 0.0696
(all data)	0.0626, 0.0737	0.0380, 0.0748
$(\Delta\rho)_{max}$, $(\Delta\rho)_{min}$/e Å^{-3}	0.402, −0.439	0.410, −0.395

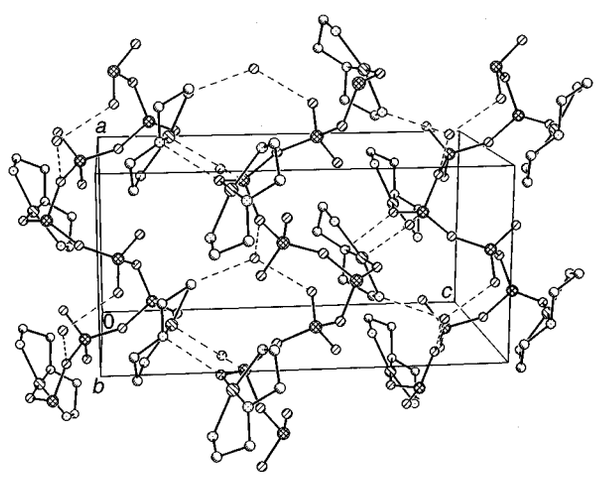

Fig. 2 Crystal packing of compound **1** viewed approximately normal to the crystallographic *bc* plane. The hydrogen atoms are omitted for clarity.

The Cu(dien) fragments are arranged alternately on each side of the vanadium oxide chain. The copper atom has a slightly distorted square planar geometry. The largest deviation of the atoms from the least-squares plane, defined by the N(1), N(2), N(3) and O(1) atoms, is 0.081(1) Å for N(2). The copper ion protrudes from this plane by 0.120(2) Å. The Cu–N bond distances [1.996(4)–2.014(4) Å] are in agreement with those in $[Cu_2(dien)_2Fe(CN)_6]\cdot 6H_2O$ [2.03(1) Å].[13] The Cu–O(1) bond length is comparable with those in $Cu(en)V_2O_6$, $Cu(bipy)V_2O_6$ and $Cu(bipy)_2V_2O_6$.[10] The copper atoms can also be viewed as bearing elongated octahedral arrangements, considering the axial interactions with both the O(2) from the adjacent chain [Cu···O(2) 2.485 Å] and O(5) from the same chain [Cu···O(5) 2.629 Å] (Fig. 2). The closest Cu···Cu separation between chains is 5.500 Å.

The chains are stabilized by the lattice water through extensive hydrogen bonding [O(w)···O(3) 2.849, O(w)···O(5)

Table 2 Selected bond lengths (Å) anf angles (°) for compound **1**

Cu–O(1)	1.956(3)	Cu–N(1)	1.996(4)
Cu–N(2)	2.001(4)	Cu–N(3)	2.014(4)
V(1)–O(1)	1.687(3)	V(1)–O(2A)	1.622(3)
V(1)–O(3)	1.800(3)	V(1)–O(4B)	1.766(3)
V(2)–O(5)	1.640(3)	V(2)–O(6)	1.623(4)
V(2)–O(3)	1.838(3)	V(2)–O(4A)	1.794(3)
N(1)–C(1)	1.472(7)	N(2)–C(2)	1.455(6)
N(2)–C(3)	1.501(6)	N(3)–C(4)	1.478(7)
C(1)–C(2)	1.510(7)	C(3)–C(4)	1.497(8)
O(1)–Cu–N(1)	94.80(14)	O(1)–Cu–N(2)	177.00(14)
N(1)–Cu–N(2)	84.5(2)	O(1)–Cu–N(3)	94.9(2)
N(1)–Cu–N(3)	165.6(2)	N(2)–Cu–N(3)	85.2(2)
O(2A)–V(1)–O(1)	106.8(2)	O(2A)–V(1)–O(4B)	110.7(2)
O(1)–V(1)–O(4B)	109.1(2)	O(2A)–V(1)–O(3)	109.7(2)
O(1)–V(1)–O(3)	111.3(2)	O(4B)–V(1)–O(3)	109.2(2)
O(6)–V(2)–O(5)	108.3(2)	O(6)–V(2)–O(4A)	112.5(2)
O(5)–V(2)–O(4A)	110.5(2)	O(6)–V(2)–O(3)	107.9(2)
O(5)–V(2)–O(3)	107.6(2)	O(4A)–V(2)–O(3)	109.8(2)
V(1)–O(1)–Cu	130.2(2)	V(1)–O(3)–V(2)	118.2(2)
V(1C)–O(4A)–V(2)	152.8(2)	C(1)–N(1)–Cu	109.2(3)
C(2)–N(2)–C(3)	117.8(4)	C(2)–N(2)–Cu	108.9(3)
C(3)–N(2)–Cu	106.2(3)	C(4)–N(3)–Cu	108.9(3)
N(1)–C(1)–C(2)	108.6(4)	N(2)–C(2)–C(1)	107.1(4)
N(2)–C(2)–C(1)	107.1(4)	C(4)–C(3)–N(2)	106.6(4)
N(3)–C(4)–C(3)	109.1(4)		

Symmetry code: A $x,y-1,z$; B $x+\frac{1}{2},-y+\frac{1}{2},-z+1$; C $x-\frac{1}{2},-y-\frac{1}{2},-z+1$.

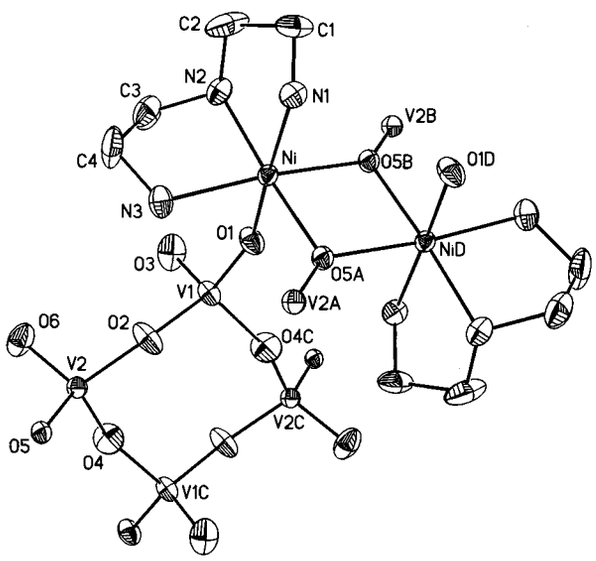

Fig. 3 The co-ordinations around the Ni and V atoms with the atomic labeling scheme (50% probability) in compound **2** with H atoms omitted for clarity.

2.821 and O(w)···N(3) 2.957 Å]. Hydrogen bond contacts are also observed within the chain [N(1)···O(5) 3.125, N(3)···O(6) 3.098 Å] and between the chains [N(2)···O(1)($-x$, $-0.5+y$, $1.5-z$) 2.854 Å].

Crystal structure of Ni(dien)V_2O_6 2

The substitution of Cu^{II} by Ni^{II} resulted in compound **2** with a remarkable structure. It forms a two-dimensional, polymeric neutral framework, where nickel(II) ions are covalently linked to the vanadium oxides.

Fig. 3 shows a thermal ellipsoid plot of the co-ordinations around the Ni and V atoms. The Ni atom has a distorted octahedral environment. It coordinates to three N atoms from the dien ligand and three O atoms from vanadium oxides. Both the Ni–N [2.066(2)–2.101(3) Å] and Ni–O [2.062(2)–2.108(2) Å] bond lengths are normal. The two vanadium atoms V(1) and V(2) are crystallographically distinct. Both have distorted

Table 3 Selected bond lengths (Å) and angles (°) for compound **2**

Ni–O(1)	2.062(2)	Ni–N(1)	2.066(2)
Ni–N(2)	2.071(3)	Ni–O(5A)	2.088(2)
Ni–N(3)	2.101(3)	Ni–O(5B)	2.108(2)
V(1)–O(3)	1.617(2)	V(1)–O(1)	1.639(2)
V(1)–O(4C)	1.791(2)	V(1)–O(2)	1.798(2)
V(2)–O(6)	1.602(2)	V(2)–O(5)	1.692(2)
V(2)–O(4)	1.780(2)	V(2)–O(2)	1.790(2)
N(1)–C(1)	1.466(4)	N(2)–C(3)	1.469(4)
N(2)–C(2)	1.473(4)	N(3)–C(4)	1.472(5)
C(1)–C(2)	1.503(5)	C(3)–C(4)	1.517(6)
O(1)–Ni–N(1)	172.86(10)	O(1)–Ni–N(2)	93.49(9)
N(1)–Ni–N(2)	82.99(10)	O(1)–Ni–O(5A)	91.39(8)
N(1)–Ni–O(5A)	92.06(9)	N(2)–Ni–O(5A)	175.04(8)
O(1)–Ni–N(3)	86.08(10)	N(1)–Ni–N(3)	99.63(11)
N(2)–Ni–N(3)	83.42(11)	O(5A)–Ni–N(3)	97.78(9)
O(1)–Ni–O(5B)	85.23(8)	N(1)–Ni–O(5B)	89.07(9)
N(2)–Ni–O(5B)	97.52(9)	O(5A)–Ni–O(5B)	82.02(8)
N(3)–Ni–O(5B)	171.29(9)	O(3)–V(1)–O(1)	109.69(12)
O(3)–V(1)–O(4C)	109.57(12)	O(1)–V(1)–O(4C)	108.31(11)
O(3)–V(1)–O(2)	109.76(12)	O(1)–V(1)–O(2)	107.61(10)
O(4C)–V(1)–O(2)	111.86(11)	O(6)–V(2)–O(5)	108.64(11)
O(6)–V(2)–O(4)	109.50(13)	O(5)–V(2)–O(4)	113.06(10)
O(6)–V(2)–O(2)	110.38(13)	O(5)–V(2)–O(2)	107.99(10)
O(4)–V(2)–O(2)	107.25(11)	V(1)–O(1)–Ni	154.79(13)
V(2)–O(2)–V(1)	129.92(13)	V(2)–O(4)–V(1C)	154.2(2)
V(2A)–O(5A)–Ni	125.65(10)	V(2A)–O(5A)–Ni(D)	132.65(10)
Ni–O(5A)–Ni(D)	97.98(8)	C(1)–N(1)–Ni	106.3(2)
C(3)–N(2)–C(2)	115.5(3)	C(3)–N(2)–Ni	107.0(2)
C(2)–N(2)–Ni	109.4(2)	C(4)–N(3)–Ni	109.3(2)
N(1)–C(1)–C(2)	108.0(3)	N(2)–C(2)–C(1)	110.7(3)
N(2)–C(3)–C(4)	109.8(3)	N(3)–C(4)–C(3)	111.7(3)

Symmetry code: A $-x+1,-y-2,-z+1$; B $x,y+1,z$; C $-x+2,-y-2,-z+1$; D $-x+1,-y-1,-z$.

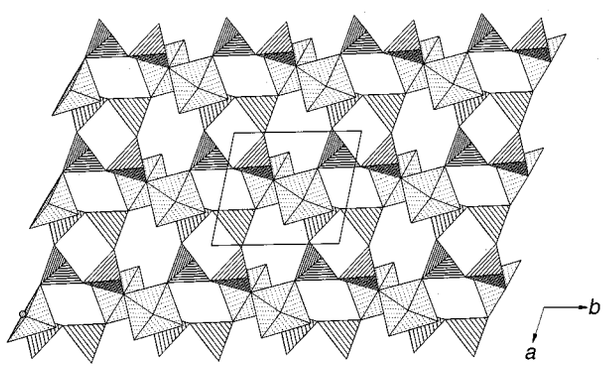

Fig. 4 Polyhedral representation of compound **2** packed along the *c* axis. All the C, H atoms are omitted for clarity.

tetrahedral geometries. They are corner-shared by O(2) and O(4) atoms to form V_4O_{12} tetramer rings instead of VO_3 chains as in the case of **1**. The V–O(2) [mean: 1.794(2) Å] and V–O(4) [mean: 1.786(2) Å] distances are close to each other. The terminal oxygen atoms O(3) and O(6) have the shortest V–O distances [1.617(2), 1.602(2) Å]. These tetramers are joined to the nickel ions through O(1) [V(1)–O(1) 1.639(2) Å] or O(5) [V(2)–O(5) 1.692(2) Å] atoms. The O(5) atom is actually three-co-ordinated, which bridges the two $Ni(dien)^{2+}$ fragments into edge-sharing $Ni_2(dien)_2(\mu\text{-}O)_2^{2+}$ dimers. There is an inversion center in the middle of the edge. Consequently, each V_4O_{12} tetramer is connected with four nickel dimers which are further linked to the other V_4O_{12} tetramers. Two-dimensional networks are thus constructed in the *ab* planes which are stacked to form channels along the [001] direction (Fig. 4). Hydrogen bondings exist within the layer [N(1)···O(1^{i}) 3.121 Å, N(2)···O(6^{ii}) 2.946, N(1)···O(3^{iii}) 3.126, N(3)···O(3^{iii}) 3.053 Å]. Only very weak interactions are found between the sheets [C(2)···O(6^{iv}) 3.245 Å] (symmetry codes: i $-x+1,-y-1,-z+1$; ii $x,y+1,z$; iii $x-1,y,z$; iv $-x+1,-y-2,-z$).

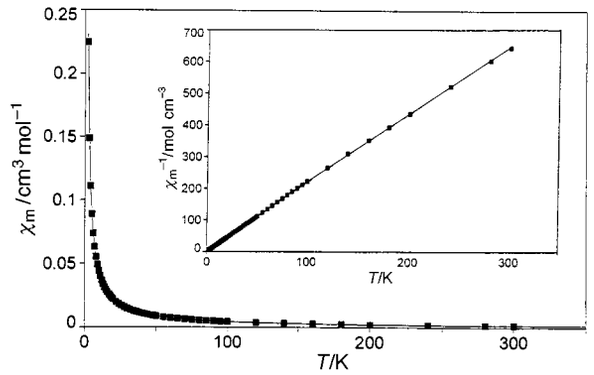

Fig. 5 The χ_m *vs.* T and $1/\chi_m$ *vs.* T plots for compound **1**.

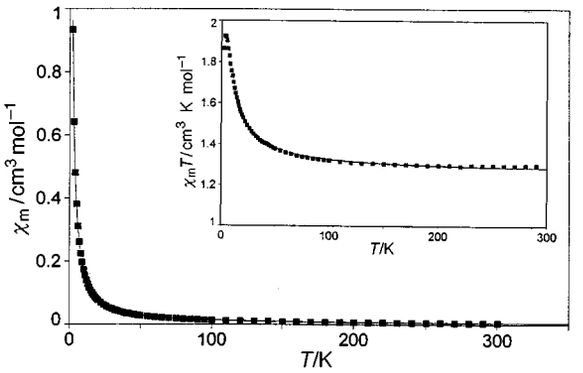

Fig. 6 The χ_m *vs.* T and $\chi_m T$ *vs.* T plots for compound **2**.

It is worth noting that the structures of compounds **1** and **2** differ significantly, though their compositions are similar. This result may originate from the natures of the transition metal ions employed. The copper(II) ion tends to have a four-co-ordinated square-planar or five-co-ordinated square pyramidal geometry due to its strong Jahn–Teller effects. The nickel(II) ion, however, favors a six-co-ordinated octahedral geometry. The novel features of the structure of **2** lie especially in the fact that its neutral frameworks are built up from both the V_4O_{12} tetramers and the nickel ions which, as we are aware, have not been observed in the vanadium oxides before. The resulted nickel "dimers" which are bridged by μ_3-O atoms exhibit interesting magnetic properties.

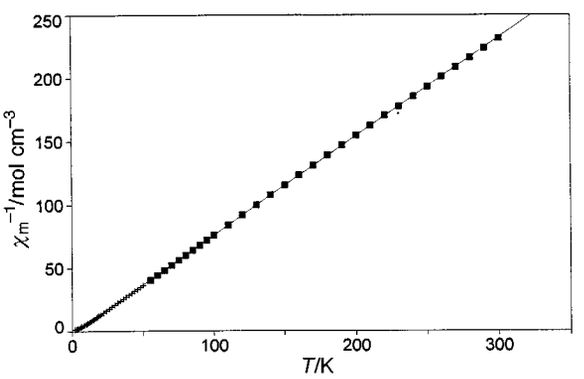

Fig. 7 The $1/\chi_m$ *vs.* T plot for compound **2**.

Magnetic properties

The temperature dependences of the magnetic susceptibilities were measured in the temperature range 300 to 2 K for both compounds **1** and **2**. Fig. 5 shows the magnetic behavior of **1** in the forms of χ_m *vs.* T and $1/\chi_m$ *vs.* T plots. At 300 K, the magnetic moment (μ_{eff}) per copper(II) atom, determined from the equation $\mu_{eff} = 2.828(\chi_m T)^{\frac{1}{2}}$, is 1.93 μ_B. The value is a little higher than that expected for an isolated paramagnetic system with $S = \frac{1}{2}$ ($\mu_{eff} = 1.73\ \mu_B$). Upon cooling to 2 K the $1/\chi_m$ *vs.* T curve is almost linear in the whole temperature range (Fig. 5), indicating principally paramagnetism in **1**. The data were therefore analysed by the Curie–Weiss law, based on eqn. (1) where N, g,

$$\chi_m = Ng^2\beta^2S(S + 1)/3k(T - \theta) \quad (1)$$

β, k have their usual meanings and θ is the Weiss constant. For $S = \frac{1}{2}$, a fit of the data, shown as the solid line in Fig. 5, led to the parameter $g = 2.16(7)$, $\theta = 0.04(1)$ K. The agreement factor R defined as $\Sigma_i[(\chi_m T)_{obs}(i) - (\chi_m T)_{calc}(i)]^2/\Sigma_i[(\chi_m T)_{obs}(i)]^2$ is equal to 3.74×10^{-6}. The g value is comparable to that obtained by EPR measurement ($g = 2.09$). The very small θ value shows that no distinct magnetic interactions exist. The paramagnetic behavior of **1** is consistent with its structure, where the copper centers are separated by the diamagnetic O–V–O–V–O moieties within the chain (Fig. 1) and O–V–O units between the adjacent chains (Fig. 2). The closest Cu · · · Cu distance is 5.5 Å between the neighboring chains. Consequently, both direct and super-exchange couplings have to be excluded.

The magnetic behavior of compound **2** is shown in Fig. 6. The magnetic moment at 300 K ($\mu_{eff} = 3.22\ \mu_B$) per nickel(II) is in accord with that expected for an isolated paramagnetic system with $S = 1$ ($\mu_{eff} = 3.25\ \mu_B$ for $g = 2.3$). On cooling from room temperature the value of $\chi_m T$ increases continuously from 1.297 cm^3 K mol^{-1} at 300 K to a maximum of 1.924 cm^3 K mol^{-1} ($\mu_{eff} = 3.93\ \mu_B$) per Ni^{II} at 3 K. Such a behavior is characteristic of a ferromagnetic coupling which is further suggested by a positive Weiss constant ($\theta = +2.852$ K) (Fig. 7). The highest value of $\chi_m T$ is consistent with that expected for a spin aligned ground state arising from the intramolecular interactions between the nickel(II) ions ($\mu_{eff} = 3.98\ \mu_B$ per Ni^{II} for $g = 2.3$). Further cooling below 3 K causes the $\chi_m T$ to decrease, reaching a value of 1.865 cm^3 K mol^{-1} at 2 K which could be due to either the zero-field splitting of the ground state or interdimer interaction. The susceptibility data were analysed using the Heisenberg Hamiltonian (2) with the theoretical eqns.[14,15] (3) and (4) where J is the coupling constant between the nickel

$$\hat{H} = -2J\hat{S}_1\cdot\hat{S}_2 - \beta(g_1\hat{S}_1 + g_2\hat{S}_2)\bar{H} \quad (2)$$

$$\chi_m = Ng^2\beta^2F(J,T)/kT \quad (3)$$

$$F(J,T) = [5 + \exp(-4J/kT)]/[5 + 3\exp(-4J/kT) + \exp(-6J/kT)] \quad (4)$$

ions. A good fit was obtained which affords the solid line in Fig. 6 with $g = 2.25(1)$, $J = 2.55(5)$ cm^{-1} and $R = 8.89 \times 10^{-5}$. The positive J value demonstrates a ferromagnetic exchange propagated between magnetic centers in **2**. The calculated g value is comparable to that obtained from EPR results (2.04). The least-squares analysis of the magnetic data is not improved when the zero-field splitting of the ground state is considered using eqns. (5)–(7). The parameters are $g = 2.25(1)$, $J = 2.55(4)$ cm^{-1}, the

$$\chi_z = \frac{Ng^2\beta^2}{kT}\cdot\frac{4\exp\left(-\frac{2D}{kT}\right) + \exp\left(\frac{D}{kT}\right) + \exp\left(-\frac{4J}{kT}\right)}{2\exp\left(-\frac{2D}{kT}\right) + 2\exp\left(\frac{D}{kT}\right) + \exp\left(\frac{2D}{kT}\right) + 3\exp\left(-\frac{4J}{kT}\right) + \exp\left(-\frac{6J}{kT}\right)} \quad (5)$$

$$\chi_x = \frac{Ng^2\beta^2}{kT} \cdot \frac{\frac{kT}{3D}\left[9\exp\left(\frac{2D}{kT}\right) - 7\exp\left(\frac{D}{kT}\right) - 2\exp\left(-\frac{2D}{kT}\right)\right] + \exp\left(-\frac{4J}{kT}\right)}{2\exp\left(-\frac{2D}{kT}\right) + 2\exp\left(\frac{D}{kT}\right) + \exp\left(\frac{2D}{kT}\right) + 3\exp\left(-\frac{4J}{kT}\right) + \exp\left(-\frac{6J}{kT}\right)} \quad (6)$$

$$\chi_m = (\chi_z + 2\chi_x)/3 \quad (7)$$

zero-field splitting energy $D = -0.05(5)$ cm^{-1} and $R = 8.85 \times 10^{-5}$.

Ginsberg *et al.*[15] have treated interdimer interaction $z'J'$ in the context of the molecular field approximation. When we take into account this interdimer interaction using equations (4) and (8)[15] the resulting parameters are $g = 2.24(8)$, $J = 2.57(2)$ cm^{-1}, $z'J' = 0.005(1)$ cm^{-1} and $R = 8.01 \times 10^{-5}$.

$$\chi_m = Ng^2\beta^2F(J,T)/[kT - 4z'J'F(J,T)] \quad (8)$$

Considering the structure of compound **2**, the ferromagnetic coupling is mainly attributed to the superexchange couplings between the nickel(II) ions through μ_3-O(5) ligands. Possible direct exchanges can be excluded because of the large Ni · · · Ni distance (3.166 Å). The Ni–O–Ni(D) angle [97.98(8)°] of the edge-sharing NiO_6 octahedra in **2** falls in the range where ferromagnetic exchange pathways should be dominant (90 ± 14°).[16] The interdimer interactions through diamagnetic V_4O_{12} tetramers, however, are expected to be very weak. The nearest Ni · · · Ni distance between the dimers is 7.226 Å. The ferromagnetic interactions observed in **2** have also been found in several other polynuclear nickel complexes. The J value for **2** is comparable to those in complexes which contain cubane nickel(II) clusters (3–26 cm^{-1})[16,17] or that in $K_6Na[Ni_3(H_2O)_3PW_{10}O_{39}(H_2O)]\cdot 12H_2O$ (2.9 cm^{-1}) which contains Ni_3 triangles.[18]

In conclusion, this work describes the structures and magnetic properties of two new polymers of vanadium oxides coordinated by transition metal complexes. The compound **1** is one dimensional and exhibits paramagnetic behavior in the temperature range 2–300 K. Compound **2** contains two-dimensional neutral sheets which are stacked to form channels along the [001] direction. Ferromagnetic exchanges are mediated through oxygen bridges between nickel ions in the layer. The results demonstrate that compounds which bear new structure types and are of magnetic interest may be obtained by the combination of different transition metal complexes with vanadium oxides.

Acknowledgements

The supports of the Natural Science Foundation of Jiangsu province (No. BK97018), the State Education Commission and the Analysis Center of Nanjing University are acknowledged. The authors are also indebted to Ms. Fen-Ling Liao and Professor Sue-Lein Wang at Tsing Hua University for X-ray intensity data collection, and Professor S. Decurtins at Bern University, Switzerland, for using the fitting program.

References

1 T. G. Chirayil, E. A. Boylan, M. Mamak, P. Y. Zavalij and M. S. Whittingham, *Chem. Commun.*, 1997, 33.
2 P. Y. Zavalij, M. S. Whittingham, E. A. Boylan, V. K. Pecharsky and R. A. Jacobson, *Z. Kristallogr.*, 1996, 464.
3 L. F. Nazar, B. E. Koene and J. F. Britten, *Chem. Mater.*, 1996, **8**, 327.
4 Y. Zhang, R. C. Haushalter and A. Clearfield, *Chem. Commun.*, 1996, 1055.
5 Y. Zhang, R. C. Haushalter and A. Clearfield, *Inorg. Chem.*, 1996, **35**, 4950.
6 Y. Zhang, C. J. O'Connor, A. Clearfield and R. C. Haushalter, *Chem. Mater.*, 1996, **8**, 595.
7 C.-Y. Duan, Y.-P. Tian, Z.-L. Lu, X.-Z. You and X.-Y. Huang, *Inorg. Chem.*, 1995, **34**,1.
8 G. Huan, J. W. Johnson, A. J. Jacobson and J. S. Merola, *J. Solid State Chem.*, 1991, **91**, 385.
9 S. Aschwanden, H. W. Schmalle, A. Reller and H. R. Oswald, *Mater. Res. Bull.*, 1993, **28**, 45.
10 J. R. D. DeBord, Y. Zhang, R. C. Haushalter, J. Zubieta and C. J. O'Connor, *J. Solid State Chem.*, 1996, **122**, 251.
11 Y. Zhang, J. R. D. DeBord, C. J. O'Connor, R. C. Haushalter, A. Clearfield and J. Zubieta, *Angew. Chem., Int. Ed. Engl.*, 1996, **35**, 989.
12 G. M. Sheldrick, SHELXTL PC, Version 5, Siemens Analytical X-Ray Instruments, Inc., Madison, WI, 1995.
13 G. O. Morpurgo, V. Mosini, P. Porta, G. Dessy and V. Fares, *J. Chem. Soc., Dalton Trans.* 1980, 1272.
14 O. Kahn, *Molecular Magnetism*, VCH, New York, 1993.
15 A. P. Ginsberg, R. L. Martin, R. W. Brookes and R. C. Sherwood, *Inorg. Chem.*, 1972, **11**, 2884.
16 A. P. Ginsberg, *Inorg. Chim. Acta*, 1971, **5**, 45 and refs. therein.
17 W. L. Gladfelter, M. W. Lynch, W. P. Schaefer, D. N. Hendrickson and H. B. Gray, *Inorg. Chem.* 1981, **20**, 2390.
18 C. J. Gomez-Garcia, E. Coronado and L. Ouahab, *Angew. Chem., Int. Ed. Engl.*, 1992, **5**, 649.

Paper 8/08839J